Contents lists available at ScienceDirect

Chemical Physics Letters

journal homepage: www.elsevier.com

Research paper

Solvent-mediated phase transformation of C_{60} crystals with well-defined hexagonal shape

Saori Yamamoto [a], Yuto Funamori [a], Yuko Kaneda [b], Makoto Tanimura [b], Masaru Tachibana [a, *]

[a] Department of Materials System Science, Yokohama City University, 22-2 Seto, Kanazawa-Ku, Yokohama 236-0027, Japan
[b] Instrumental Analysis Center, Yokohama National University, 79-5 Tokiwadai, Hodogaya-Ku, Yokohama 240-8501, Japan

ARTICLE INFO

ABSTRACT

CCl_4-solvated C_{60} crystals with hexagonal shape were grown by the liquid-liquid interfacial precipitation method with CCl_4 and toluene as poor and good solvents, respectively. Interestingly, the morphology of the hexagonal crystals with the growth liquid are drastically changed with drying in air. A lot of fine rod crystals appear over the original crystals with air-drying, whereas the hexagonal outline of the original crystals is kept even after the transformation. Such change in the morphology is explained by the solvent-mediated phase transformation due to the dissolution of the original crystals by toluene and then re-precipitation of the rod crystals.

1. Introduction

Fullerene crystals of C_{60} and C_{70} have attracted much attention due to their physical and chemical properties [1]. The properties strongly depend on not only crystal structure but also size and shape. Various growth methods have been developed to produce unique forms of fullerene crystals. Recent studies have focused on solvated crystals with small sizes from micrometers to nanometers. Actually many nano/microcrystals with various shapes called nanowhiskers [2–5], nanosheets [6–8], nanowires [9,10], nanorods [11], nanoballs [12], nanocubes [13] have been grown from the solution. They can be transformed into different shapes by solvent treatments after the growth [14,15]. Such solvent treatments can also produce interesting hierarchical architectures which show fascinating properties and applications such as sensing [16,17].

Among various solution methods for the preparation of fullerene nano/microcrystals, a liquid-liquid interfacial precipitation (LLIP) method [2,5], using a mixture of solvents consisting of a good solvent and a poor solvent, shows great potential in the morphology control of fullerene crystals because of its facileness and versatility [18–20]. It is known that the solvents play a crucial role in the morphology control or crystalline determination of the fullerene crystals. The subtle variation of the solvent types or solvent ratios can remarkably change the morphological features of the products [21,22]. Thus it is expected that unique shapes and properties of nano/microcrystals can be further produced by the proper selection and combination of solvents.

In the LLIP method, the difference in the solubility of fullerene for two solvents used is important for the precipitation of crystals. So far, the kind of good solvent used has been mainly changed for the growth of nano/microcrystals. On the other hand, alcohols have been usually employed as poor solvents or precipitants. Thus, the selection of poor solvent except for alcohols is of very interest for the growth of novel nano/microcrystals.

In this paper, we report the growth of C_{60} crystals by using carbon tetrachloride (CCl_4) as poor solvent in the LLIP method with C_{60}-saturated toluene solution. The obtained crystals are CCl_4-solvated C_{60} crystals with hexagonal shapes. Interestingly, the morphologies of the crystals are drastically changed with drying in air. A lot of fine rod crystals appear in the hexagonal crystals with air-drying, whereas the hexagonal outline of the original crystals is kept even after the transformation. The long axes of the rod crystals are arranged to be parallel to one of the sides of the original hexagonal outline. This means that the hexagonal symmetry of the original crystals is passed down to the orientation of the rod crystals through the transformation. It is shown that such unique morphology is formed by the solvent-mediated phase transformation in which the dissolution of the original crystals by toluene and then re-precipitation of the rod crystals occur. The unique

* Corresponding author.
Email address: tachiban@yokohama-cu.ac.jp (M. Tachibana)

https://doi.org/10.1016/j.cplett.2019.05.047
Received 20 April 2019; Received in revised form 27 May 2019; Accepted 28 May 2019
Available online xxx
0009-2614/

morphology after the transformation also correspond to a kind of hierarchical architecture.

2. Experimental procedure

2.1. Sample preparation

C_{60} powder with a purity of more than 99.95% was purchased from MTR Ltd., USA. The solvents, toluene and CCl_4 were purchased from FUJIFILM Wako Pure Chemical Corporation, Japan. The solvents were used as received without further purification. Toluene solution saturated with C_{60} was prepared as follows. The C_{60} powder was crushed in a mortar using a pestle for 30 min to facilitate dissolution of C_{60} powder into the toluene solution. The crushed C_{60} powder was dissolved in toluene with the assistance of ultrasonic oscillating for 30 min at 5 °C. Then the solution was filtered in order to remove the undissolved C_{60} powder. Such C_{60}-saturated toluene solution prepared in above procedure was kept for 24 h at 5 °C. On the other hand, CCl_4 as a poor solvent was also kept at 5 °C to avoid the gradient of growth temperature.

Using these solutions, C_{60} crystals were grown by the LLIP method in below procedure [2,5]. First, the CCl_4 as a poor solvent was put into a glass bottle. Next, the toluene solution saturated with C_{60} was gently added to form a liquid-liquid interface (toluene solution saturated with C_{60}:CCl_4 = 1:2 (v:v)) (Fig. S1(a)). The bottle was capped and kept for several seconds without any disturbances, and then shaken up by hand (Fig. S1(b)). The obtained mixture of solutions was stored at 5 °C in an incubator for 24 h so that C_{60} crystals were precipitated (Fig. S1(c)).

2.2. Characterization

The obtained C_{60} crystals were dropped on a glass-slide. The *in-situ* observation of the crystals with air-drying was carried out by using an optical microscope (Olympus, BX50). In other measurements, C_{60} crystals were dropped on a glass-slide and dried at 23 °C to remove the mother liquid. After drying, they were characterized. The compositions in the crystals were examined by means of Fourier transform infrared spectroscopy (FT-IR, JASCO, FT/IR-4100) with the attenuated total reflection (ATR PRO ONE, JASCO) and thermogravimetry (TG, Hitachi High-Technologies, STA7300) at a heating rate of 10 °C/min under N_2 gas flow (200 mL/min). The crystal structure and orientations of the crystals were examined by using X-ray diffractometer (XRD, Bruker, D8 Advance) with Cu-Kα radiation (λ = 1.5418 Å), and transmission electron microscopy (TEM, JEOL, JEM-2100F and JEM-1010) operated at 100 kV and 200 kV.

3. Results and discussion

3.1. Morphological transformation

Fig. 1(a) shows an as-grown crystal on the glass-slide just after taking it out of the solution. Note that the crystal is still covered by the mother liquid consisting of the mixture of toluene and CCl_4. As seen in Fig. 1(a), it exhibits a hexagonal shape with the length of the diagonal line of 50 μm and the thickness of 5 μm. Interestingly, the morphology of the hexagonal crystal is drastically changed with air-drying at 23 °C as shown in Fig. 1(b)–(d) (Video S1). Such change is accomplished after several 10 s. It should be noted that a lot of fine rod crystals appear in the original crystal, whereas the hexagonal outline of the original crystal is kept even after the transformation. The long axes of the rod crystals are arranged to be parallel to one of the edges of the original hexagonal outline. The orientations of the rod crystals are classified into three kinds of ones with a relative angle of 60° to each other. Thus, the hexagonal symmetry of the original crystals is passed down to the orientation of the rod crystals through the transformation. Such morphology after the transformation exhibits a kind of hierarchical architecture.

To examine such morphological transformation in more detail, additional samples were prepared by solvent treatments for as-grown ones. It is well-known that the morphology of solvated crystals of C_{60} depends on the solvent. According to previous reports, the morphologies of C_{60} crystals grown from toluene and CCl_4 solutions exhibits rod and hexagonal shapes, respectively [5,6,23,24]. It is speculated that the rod and hexagonal crystals observed in this study are related to C_{60} crystals solvated with toluene and CCl_4, respectively. Therefore, it is supposed that the toluene greatly affects the transformation of the hexagonal crystals into the rod crystals in this study. It is expected that the morphological transformation can be promoted by introducing toluene or hindered by removing toluene.

To confirm these, additional CCl_4 was dropped on the as-grown crystal covered by the mother liquid before the transformation. By this treatment, the concentration of toluene on the as-grown crystal is reduced or removed. Consequently CCl_4 becomes predominant on the as-grown crystal. After several seconds, the liquid on the as-grown crystal is perfectly evaporated with air-drying. As a result, no morphological transformation occurs even after the evaporation (Fig. 2(b)), in contrast with the drastic transformation as shown in Fig. 1. The morphology of the as-grown crystal remained almost unchanged even after the evaporation. This can be attributed to the suppression of the effect of toluene due to the dropping of additional CCl_4. Thus, we can obtain the as-grown crystals which are stable even in air-drying. Such stable as-grown crystals are called “hexagonal” crystals after.

On the other hand, the morphological transformation, as similar to that in Fig. 1, is observed when a slight amount of toluene is dropped on the as-grown crystal. The transformation rate is a little fast compared with that in Fig. 1. Moreover, similar transformation also occur even for the “hexagonal” sample when a slight amount of toluene is dropped on the sample. (Fig. 2(c)). It is therefore obvious that the toluene promotes the morphological transformation.

The results of the morphological transformations as mentioned above are summarized in Fig. 2. The relationship among typical three samples before and after the transformation are also shown with the treatments. The three samples are (a) as-grown crystal covered by the mother liquid, (b) hexagonal crystal dried in air, and (c) rod crystal

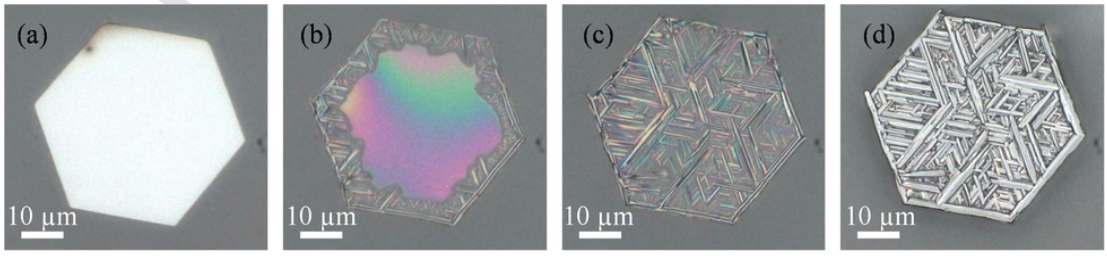

Fig. 1. Serial micrographs of the morphological transformation of the obtained crystal on the glass substrate with air-drying at 23 °C. (a) As-grown crystal which is covered by the mother liquid, (b) Partially transformed crystal, (c) Almost perfectly transformed crystal, (d) Perfectly dried crystal.

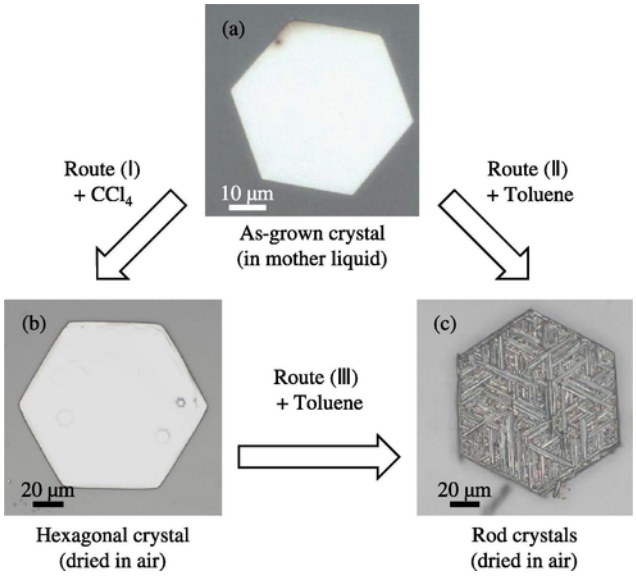

Fig. 2. Correlation diagram of specific crystals obtained by the treatments with CCl_4 and toluene. (a) shows the as-grown crystal covered with the mother liquid, corresponding to Fig. 1(a). (b) and (c) show the hexagonal crystal and the rod crystal dried in air after treated with CCl_4 and toluene for (a) as-grown crystals, respectively. Note that the crystals shown in the figure are obtained from different original crystals.

dried in air. The route (I) corresponds to the stabilization of the as-grown crystal from as-grown sample with the growth solution, which is unstable in air, to the hexagonal one, which is stable in air, due to the addition of CCl_4. The routes (II) and (III) correspond to the morphological transformations from the as-grown and hexagonal ones to the rod sample due to the addition of a little toluene, respectively. Thus, the morphology can be controlled by these treatments with solvents such as toluene and CCl_4. It is expected that the change in the morphology can be related to so-called solvent-mediated phase transformation as has been reported for various crystals so far [25].

Similar change in the morphology has been observed for well-known methanofullerene crystals [26]. The transformation is occurred by thermal annealing around 160 °C. Therefore, it is considered that the transformation mechanism induced by the heat-treatment is different from that associated with two kind of solvents such as toluene and CCl_4 at lower temperature of 23 °C in this study.

To clarify the mechanism of the transformation in this study, the hexagonal and rod crystals before and after the transformation were examined by FT-IR, TG, XRD, TEM, and X-ray topography. First, to examine the solvation in the crystal, FT-IR and TG are measured.

3.2. Composition analysis

Fig. 3 shows FT-IR spectra of the hexagonal crystals and the rod crystals before and after the transformation, respectively, taken at 23 °C in air. They were measured with ATR prism which is made of ZnSe. For references, FT-IR spectra of toluene, CCl_4 and C_{60} powder are also included in Fig. 3. For the hexagonal crystals before the transformation, clear peaks are observed at around 759, 782, 1181, 1428 cm^{-1}. Comparing with those of CCl_4 and C_{60} powder, the peaks at around 1181, 1428 cm^{-1} are assigned to those of C_{60}. The other peaks at around 759, 782 cm^{-1} are associated with those of CCl_4. This means that the hexagonal crystals are solvated crystals consisting of C_{60} and CCl_4 as expected. On the other hand, in the rod crystals, some new peaks at around at 700 and 725 cm^{-1} are observed in addition to those observed for the hexagonal crystals. Comparing with the spectrum of toluene, these new peaks can be assigned to those of toluene. This means that the rod crystals are also solvated crystals composing of C_{60},

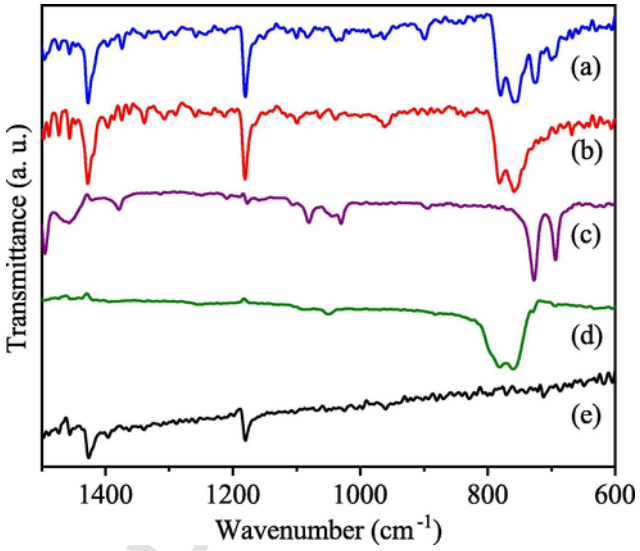

Fig. 3. FT-IR spectra of (a) rod crystals, (b) hexagonal crystals, (c) toluene, (d) CCl_4 and (e) C_{60} powder.

toluene and CCl_4. Thus the hexagonal crystals before the transformation contain only CCl_4 as solvent, whereas the rod crystals after the transformation contains not only CCl_4 but also toluene. From these results, it is suggested that the incorporation of toluene into the crystal gives rise to the morphological transformation.

Fig. 4 shows TG curves of the hexagonal and rod crystals. The measurements were performed at a heating rate of 10 °C/min under a N_2 gas flow (200 mL/min). For the hexagonal crystals, the weight loss of about 29.0% is observed between 97 and 133 °C as seen in Fig. 4. According to the FT-IR analysis as mentioned above, the hexagonal crystals contain only CCl_4 as solvent. Therefore, the weight loss is due to desorption of CCl_4. From the analysis of the weight loss with molecular weights of 720.66 and 153.82 for C_{60} and CCl_4, respectively, the composition formula is obtained to be $C_{60} \cdot 2CCl_4$ with 1:2 composition.

On the other hand, in the rod crystals, the weight loss of about 10.8% is observed between 120 and 188 °C which are a little higher than those in the hexagonal ones as mentioned above. According to the FT-IR analysis as mentioned above, the rod crystals contain not only CCl_4 but also toluene. It is therefore considered that the weight loss is ascribed to desorption of two kind of solvents such as CCl_4 and toluene, although it is difficult to evaluate the composition ratio of the solvents

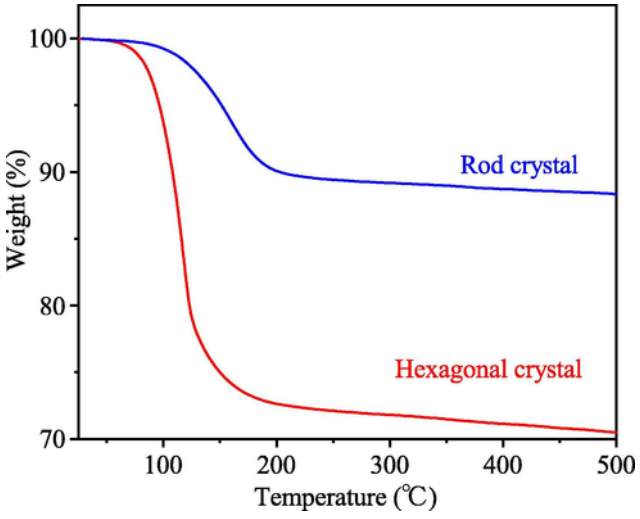

Fig. 4. TG curves of rod crystals and hexagonal crystals.

from the TG curve. It is known that the boiling point of toluene is 111 °C which is higher than 77 °C of CCl_4. Thus, the high temperature for the weight loss in the rod crystals can be mainly due to the high boiling point of toluene. Moreover, it should be noted that the weight loss of 10.8% in the rod crystals is much smaller than 29.0% in the hexagonal crystal. This means that the solvent content in the rod crystals is small compared with that in the hexagonal crystals. Thus it is suggested that desorption of CCl_4 in the crystal occurs with the incorporation of toluene during the transformation.

In the case of C_{60} • CCl_4 complex with smaller 1:1 composition, it is expected that the weight loss is reduced to 17.6%. However, the value is still larger than 10.8% observed in the rod crystals in Fig. 4. In the case of C_{60} • toluene complex in which CCl_4 in C_{60}•CCl_4 as mentioned above is replaced by toluene with smaller molecular weight of 92.14, it is anticipated that the weight loss is further reduced to 11.3%. The value is in good agreement with that observed in the rod crystals. Actually, the rod crystals include not only toluene but also CCl_4 according to the FT-IR analysis. Thus, in the rod crystals, it is predicted that the composition ratio of toluene to C_{60} is further less than 1.0. From such analysis, a composition ratio of C_{60}:CCl_4:toluene with 1:0.2:0.6 is suggested as a compound corresponding to the weight loss of 10.8% observed in the rod crystals in Fig. 4.

3.3. Crystal structure and orientations

Fig. 5 shows XRD patterns of the hexagonal and rod crystals before and after the morphological transformation, respectively. The XRD pattern of rod crystals is quite different from that of hexagonal crystals. This implies that the crystal structure in the rod crystals is different from that in the hexagonal crystals. Thus the morphological transformation is associated with the change in the crystal structure.

The XRD pattern of the hexagonal crystals is assigned to a hexagonal structure with lattice constants of a = 10.165 Å and c = 10.810 Å. These crystal parameters are in good agreement with those of CCl_4-solvated C_{60} crystals reported previously [6,23]. This is consistent with the fact that the as-grown hexagonal crystals contain only CCl_4 as solvent. On the other hand, the XRD pattern of the rod crystals is analyzed, and assigned to a monoclinic structure with lattice constants of a = 17.630 Å, b = 10.181 Å, c = 10.946 Å and β = 116.40°. These crystal parameters are slightly different from those of toluene-solvated C_{60} crystals reported previously [27], although both crystals exhibit a monoclinic structure. The discrepancy in the crystal parameters can be attributed to the fact that the rod crystals contains not only toluene but also CCl_4 as solvents. This also suggests that our rod crystals exhibit a specific solvated structure in which the toluene in the toluene-solvated C_{60} crystals reported previously [27] might be partially replaced with CCl_4.

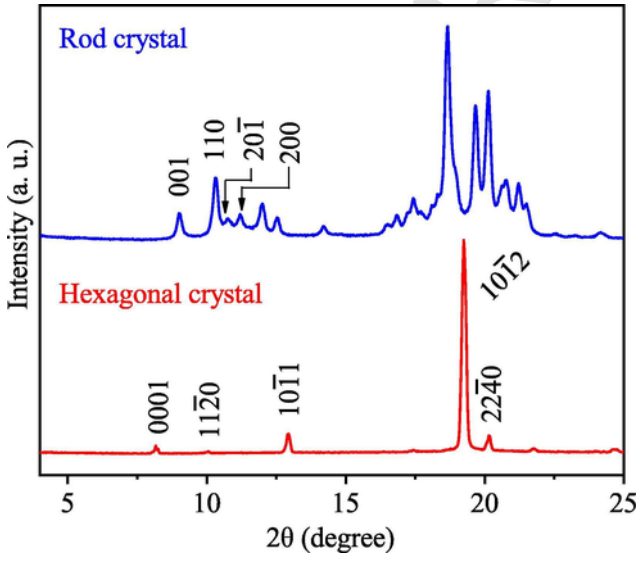

Fig. 5. XRD patterns of rod crystals and hexagonal crystals.

To clarify the relative orientations of the crystals, TEM images and its selected area electron diffraction (SAED) patterns are observed for the hexagonal crystals and the monoclinic rod crystals before and after the transformation. Fig. 6(a) shows TEM image of the hexagonal crystal before the transformation. The corresponding SAED pattern from the area surrounded with a red squire in Fig. 6(a) is shown in the inset. The SAED pattern exhibits clear isolated spots corresponding to a single crystal with hexagonal symmetry. All spots in the SAED pattern are indexed according to the hexagonal structure. This is consistent with the hexagonal structure by XRD analysis as mentioned above.

On the other hand, TEM image and SAED pattern of the rod crystals after the transformation are shown in Fig. 6(b). The TEM exhibits a part of the hexagonal aggregation consisting of the rod crystals. Fig. 6(c) shows TEM image and SAED pattern of one rod crystal which is selected from the rod crystals in red square in Fig. 6(b). The SAED pattern from the red circle in the rod crystal is shown in the inset of Fig. 6(c). The SAED pattern exhibits clear isolated spots corresponding to a single crystal, which can be assigned to a monoclinic structure. The angle between (2 0 0) and (0 0 1) is 116°, which is in good agreement with that by XRD analysis as mentioned above. In addition, other SAED patterns from different directions are observed (Fig. S2). The d-spacing of 7.8 Å, 8.7 Å and 5.1 Å corresponding to main spots are (2 0 0), (1 1 0) and (0 2 0), which are also in good agreement with those by XRD analysis as mentioned above. Comparing with the SAED pattern with that of the hexagonal crystal in Fig. 6(a), it is found that the a-c plane ((0 1 0) basal plane) in one rod crystal with the monoclinic structure is associated with a-b plane ((0 0 0 1) basal plane) of the hexagonal crystal.

Moreover, the SAED pattern from the area including three kinds of the rod crystals with different orientations as mentioned above exhibits unique complex pattern as seen in Fig. 6(b). The pattern shows the superposition of three identical subpatterns corresponding to the monoclinic structure as shown in Fig. 6(c). The lattices of the three subpatterns are also drawn with different colors on the extended SAED pattern in Fig. 6(d). It is obvious that the lattices are completely coincident with diffraction spots. The three diffraction subpatterns form a relative angle of 60° to each other. This geometrical relationship among three directions is the same with that among the rod crystals after the transformation as mentioned above.

From the analysis of SAED pattern as mentioned above, the relative orientations between the lattices of the hexagonal crystal and the monoclinic rod crystal before and after the transformation can be drawn as shown in Fig. 7. The directions of [1 0 0] in the rod crystals are arranged to be parallel to one of three identical directions of $\langle 1\ \bar{1}\ 0\ 0 \rangle$ in the hexagonal crystal. It should be noted that the periodicity of [1 0 0] direction in the monoclinic rod crystal after the transformation is in good agreement with that of $\langle 1\ \bar{1}\ 0\ 0 \rangle$ in the as-grown hexagonal crystal. It is considered that this agreement in the periodicity is the reason why the hexagonal crystals have passed down their hexagonal symmetry to the orientation of the rod crystals during the transformation. The outline of the aggregation of the rod crystals also exhibits the hexagonal shape of the original crystal.

To evaluate the crystal perfection of the rod crystal after the transformation, X-ray topography by using synchrotron radiation at KEK-PF was applied for the aggregation of the rod crystals with well-defined hexagonal outline (Fig. S3(a)). The hexagonal outline of the aggregation of the rod crystals is clearly observed in the X-ray topography (Fig. S3(b)), although it is difficult to resolve individual rod crystals due to the resolution limit. The clear image of the hexagonal outline

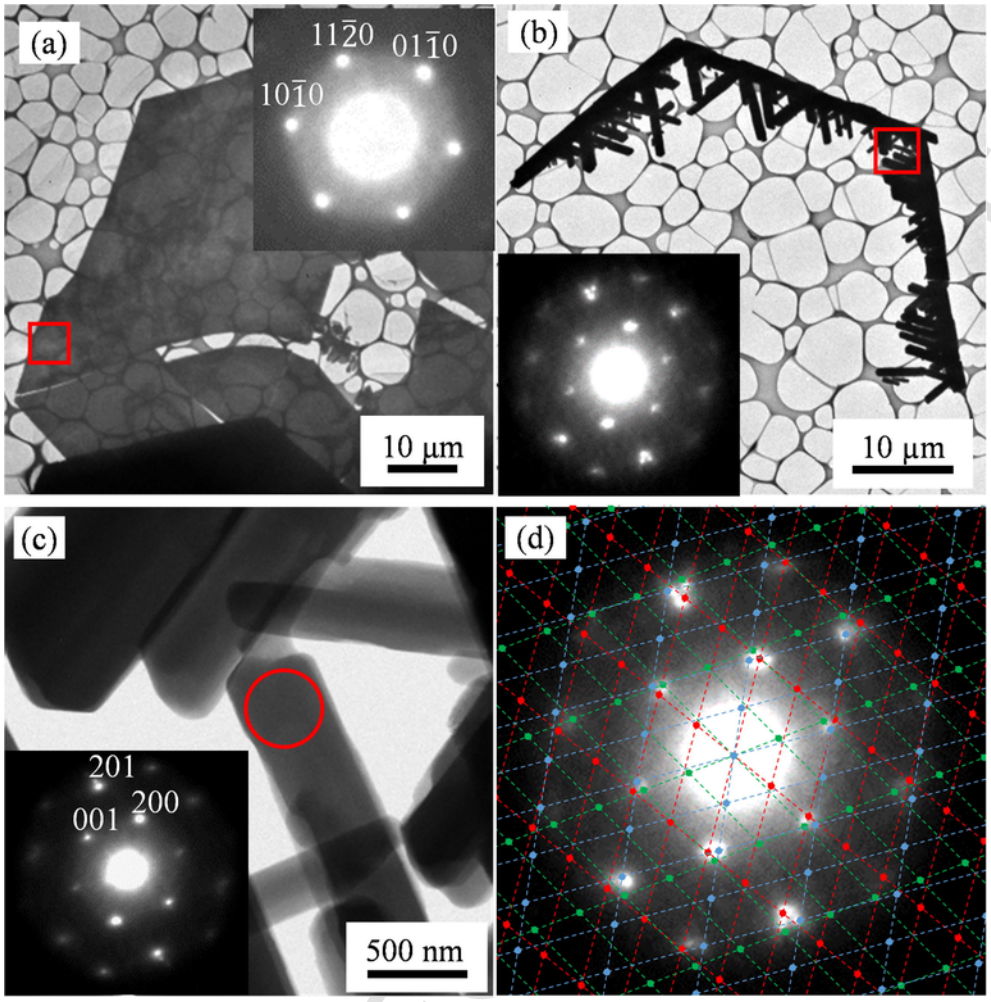

Fig. 6. TEM images and SAED patterns of (a) hexagonal crystal and (b) monoclinic rod crystals with three different orientations. (c) shows TEM image and SAED pattern from one monoclinic rod crystal in (b). (d) shows an extended figure of the SAED in (b) on which three identical lattices corresponding to (c) are drawn with a relative angle of 60° to each other.

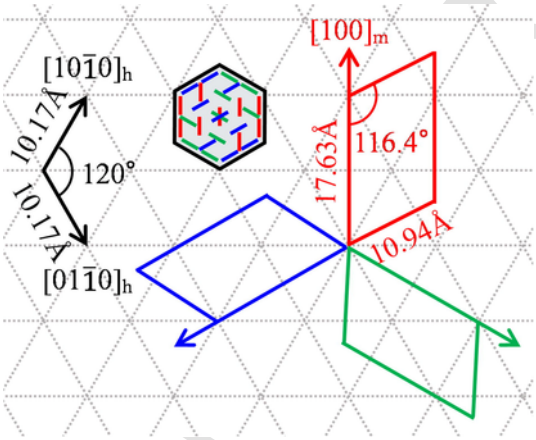

Fig. 7. Schematic representation of the relative orientations between the lattices of the hexagonal crystals and monoclinic rod crystals before and after the transformation.

means that the rod crystals oriented to three directions as mentioned above are uniformly distributed over the original crystal, and have high crystallinity even after the transformation.

Finally, we suggest phase transformation mechanism as shown in Fig. 8. The as-grown crystal is covered with the mother liquid which contain CCl_4 and toluene solution as soon as they are picked up from the growth bottle. First, the CCl_4 in the mother liquid is evaporated faster than toluene in open air, since the boiling point of 77 °C for CCl_4 is lower than 111 °C of toluene. Then, the toluene becomes dominant in the mother liquid. As a result, the as-grown hexagonal C_{60} crystal is partially dissolved in the toluene as the mother liquid, since the solubility of C_{60} in the toluene is 2.9 mg/mL [28] which is much high compared with 0.32 mg/mL in CCl_4 [29]. After that, the C_{60}-dissolved toluene solution gets saturated by the evaporation of toluene with air-drying. Consequently a lot of fine rod crystals are re-precipitated from the C_{60}-supersaturated toluene solution. In these processes, a part of CCl_4 in the crystals is desorbed with the incorporation of toluene. As a result, the rod crystals solvated with CCl_4 and toluene molecules are formed.

As mentioned above, the [1 0 0] directions in the monoclinic rod crystals are arranged to be parallel to one of three identical directions of $\langle 1\ \bar{1}\ 0\ 0\rangle$ in the original hexagonal crystal. The re-precipitation with such arrangement is attributed to the good agreement of the periodicity of the [1 0 0] direction in the monoclinic rod crystals with that of the $\langle 1\ \bar{1}\ 0\ 0\rangle$ directions in the as-grown hexagonal crystals. Thus, the hexagonal symmetry of the original crystals is passed down to the orientation of the rod crystals through the transformation.

Most recently, similar transformation has been reported for hexagonal crystals obtained from the solution of C_{60} in CCl_4 and *m*-xylene mixture [30]. The transformation mechanism should be similar to that in this work, although the good solvent (*m*-xylene) used and the crystal

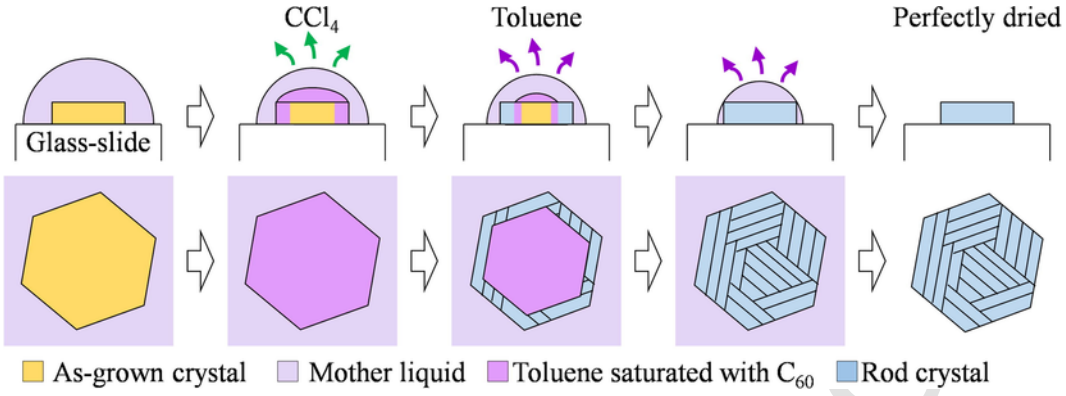

Fig. 8. Schematic representation of the morphological transformation.

structure (hexagonal close-packed structure) in the rod crystals are different from those in this work. Our results demonstrate that such solvent-mediated phase transformation is more useful for the control of more complicated crystal morphology.

4. Conclusion

We have shown the growth of unique CCl_4-solvated C_{60} crystals with hexagonal shape by the LLIP method using CCl_4 and toluene as poor and good solvents, respectively. It was found that the morphology of the hexagonal crystals with the growth liquid are drastically changed with air-drying. A lot of fine rod crystals appear over the original crystals with air-drying, whereas the hexagonal outline of the original crystals is kept even after the transformation. The hexagonal symmetry of the original crystals is passed down to the orientation of the rod crystals through the transformation. Such unique morphology after the transformation is attributed to the good agreement in the periodicity in a crystallographic direction for solvated crystals before and after the transformation. Moreover, it was shown that the dissolution of the original crystals by toluene and then re-precipitation of the rod crystals occur in the transformation process. Such solvent-mediated phase transformation is useful for the growth of novel nano/microcrystals.

Declaration of Competing Interest

The authors declared that there is no conflict of interest.

Acknowledgments

We thank Dr. H. Murata for the helpful discussion for sample preparation and characterization. X-ray topography was performed in BL20B at the Photon Factory (PF) of the High Energy Accelerator Research Organization (KEK) under the approval of the Program Advisory Committee (Proposal No. 2017G087). This study was supported by Iketani Science and Technology Foundation (0291078-A) and JSPS KAKENHI (17K06797).

Appendix A. Supplementary material

Supplementary data to this article can be found online at https://doi.org/10.1016/j.cplett.2019.05.047.

Supplementary video 1

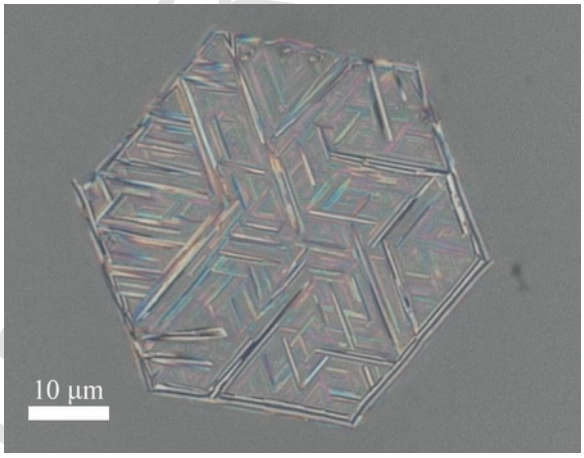

References

[1] M.S. Dresselhaus, G. Dresselhaus, P.C. Eklund, Science of Fullerenes and Carbon Nanotubes, Academic Press, San Diego, 1996.
[2] K. Miyazawa, Y. Kuwasaki, A. Obayashi, M. Kuwabara, C_{60} nanowhiskers formed by the liquid – liquid interfacial precipitation method, J. Mater. Res. 17 (2002) 83–88.
[3] M. Tachibana, K. Kobayashi, T. Uchida, K. Kojima, M. Tanimura, K. Miyazawa, Photo-assisted growth and polymerization of C_{60} 'nano' whiskers, Chem. Phys. Lett. 374 (2003) 279–285.
[4] K. Kobayashi, M. Tachibana, K. Kojima, Photo-assisted growth of C_{60} nanowhiskers from solution, J. Cryst. Growth 274 (2005) 617–621.
[5] K. Miyazawa, Y. Ochiai, M. Tachibana, T. Kizuka, S. Nakamura, Fullerene Nano-Whiskers, second ed., Pan Stanford Pub, 2019.
[6] M. Sathish, K. Miyazawa, Size-tunable hexagonal fullerene (C_{60}) nanosheets at the liquid-liquid interface, J. Am. Chem. Soc. 129 (2007) 13816–13817.
[7] T. Wakahara, M. Sathish, C. Hu, Y. Tateyama, Y. Nemoto, T. Sasaki, O. Ito, Preparation and optical properties of fullerene/ferrocene hybrid hexagonal nanosheets and large-scale production of fullerene hexagonal nanosheets, J. Am. Chem. Soc. 131 (2009) 9940–9944.
[8] K. Osonoe, R. Kano, M. Tachibana, Synthesis of C_{70} two-dimensional nanosheets by liquid – liquid interfacial precipitation method, J. Cryst. Growth 401 (2014) 458–461.
[9] J.F. Geng, W.Z. Zhou, P. Skelton, W.B. Yue, I.A. Kinloch, A.H. Windle, B.F.G. Johnson, Crystal structure and growth mechanism of unusually long fullerene (C_{60}) nanowires, J. Am. Chem. Soc. 130 (2008) 2527–2534.
[10] C. Park, H.J. Song, H.C. Choi, The critical effect of solvent geometry on the determination of fullerene (C_{60}) self-assembly into dot, wire and disk structures, Chem. Commun. (2009) 4803–4805.
[11] M. Yao, B.M. Andersson, P. Stenmark, B. Sundqvist, B. Liu, T. Wa, Synthesis and growth mechanism of differently shaped C_{60} nano/microcrystals produced by evaporation of various aromatic C_{60} solutions, Carbon 47 (2009) 1181–1188.
[12] A. Masuhara, Z. Tan, H. Kasai, H. Nakanishi, H. Oikawa, Fullerene fine crystals with unique shapes and controlled size, Jpn. J. Appl. Phys. 48 (2009) 0502061–0502063.
[13] C. Park, E. Yoon, M. Kawano, T. Joo, H.C. Choi, Self-crystallization of C_{70} cubes and remarkable enhancement of photoluminescence, Angew. Chem. Int. Ed. 49 (2010) 9670–9675.
[14] M. Sathish, K. Miyazawa, J.P. Hill, K. Ariga, Solvent engineering for shape-shifter pure fullerene (C_{60}), J. Am. Chem. Soc. 131 (2009) 6372–6373.

[15] A. Masuhara, Z. Tan, M. Ikeshima, T. Sato, H. Kasai, H. Oikawa, H. Nakanishi, Cyclic transformation in shape and crystal structure of C_{60} microcrystals, CrystEngComm. 14 (2012) 7787–7791.

[16] P. Bairi, K. Minami, W. Nakanishi, J.P. Hill, K. Ariga, L.K. Shrestha, Hierarchically structured fullerene C_{70} cube for sensing volatile aromatic solvent vapors, ACS Nano 10 (2016) 6631–6637.

[17] S. Zheng, M. Xu, X. Lu, Facile method toward hierarchical fullerene architectures with enhanced hydrophobicity and photoluminescence, ACS Appl. Mater. Interfaces 7 (2015) 20285–20291.

[18] L.K. Shrestha, Y. Yamauchi, J.P. Hill, K. Miyazawa, K. Ariga, Fullerene crystals with bimodal pore architectures consisting of macropores and mesopores, J. Am. Chem. Soc. 135 (2013) 586–589.

[19] L.K. Shrestha, R.G. Shrestha, J.P. Hill, T. Tsuruoka, Q. Ji, T. Nishimura, K. Ariga, Surfactant-triggered nanoarchitectonics of fullerene C_{60} crystals at a liquid – liquid interface, Langmuir 32 (2016) 12511–12519.

[20] B. Wang, S. Zheng, A. Saha, L. Bao, X. Lu, D.M. Guldi, Understanding charge-transfer characteristics in crystalline nanosheets of fullerene/(metallo)porphyrin cocrystals, J. Am. Chem. Soc. 139 (2017) 10578–10584.

[21] J. Kim, C. Park, H.C. Choi, Selective growth of a C_{70} crystal in a mixed solvent system: from cube to tube, Chem. Mater. 27 (2015) 2408–2413.

[22] S. Zheng, N.T. Cuong, S. Okada, T. Xu, W. Shen, X. Lu, K. Tsukagoshi, Solvent-mediated shape engineering of fullerene (C_{60}) polyhedral microcrystals, Chem. Mter. 30 (2018) 7146–7153.

[23] R. Ceolin, V. Agafonov, D. Andre, A. Dworkin, H. Szwarc, J. Dugue, B. Keita, L. Nadjo, C. Fabre, A. Rassat, Fullerene C60, 2CC14 solvate. A solid-state study, Chem. Phy. Lett. 208 (1993) 259–262.

[24] S. Ogawa, H. Furusawa, T. Watanabe, H. Yamamoto, Observation of condensed of C60 assembled from solution, J. Phys. Chem. Solids 61 (2000) 1047–1050.

[25] S. Wu, M. Chen, K. Li, S. Xu, B. Yu, S. Liu, B. Hou, J. Gong, Solvent penetration mediated phase transformation for the preparation of aggregated particles with well-defined shape, CrystEngComm. 18 (2016) 9223–9226.

[26] L. Zheng, Y. Han, Solvated crystals based on [6,6]-phenyl-C_{61} -butyric acid methyl ester (PCBM) with the hexagonal structure and their phase transformation, J. Phys. Chem. B 116 (2012) 1598–1604.

[27] M.V. Korobov, E.B. Stukalin, A.L. Mirakyan, I.S. Neretin, Y.L. Slovokhotov, A.V. Dzyabchenko, A.I. Ancharov, B.P. Tolochko, New solid solvates of C_{60} and C_{70} fullerenes: the relationship between structures and lattice energies, Carbon 41 (2003) 2743–2755.

[28] W.A. Scrivens, J.M. Tour, Potent solvents for C_{60} and their utility for the rapid acquisition of ^{13}C NMR data for fullerenes, J. Chem., Soc. Chem. Commun. 3 (1993) 1207–1209.

[29] R.S. Ruoff, D.S. Tse, R. Malhotra, D.C. Lorents, Solubility of C_{60} in a variety of solvents, J. Phys. Chem. 97 (1993) 3379–3383.

[30] Y. Lei, S. Wang, Z. Lai, X. Yao, Y. Zhao, H. Zhang, H. Chen, Two-dimensional C60 nano-meshes via crystal transformation, Nanoscale (in press).